

# Synthesis, Crystal Structure, and Second-Order Nonlinear Optical Properties of a New Bis(salicylaldiminato)nickel(II) Metal Complex

Frédéric Averseng, Pascal G. Lacroix,\* Isabelle Malfant, Géraldine Lenoble, and Patrick Cassoux

*Laboratoire de Chimie de Coordination du CNRS, 205 route de Narbonne, 31077 Toulouse Cedex, France*

Keitaro Nakatani, Isabelle Maltey-Fanton, and Jacques A. Delaire

*PPSM, CNRS URA 1906, Ecole Normale Supérieure de Cachan, Avenue du Président Wilson, 94235 Cachan Cedex, France*

Ally Aukauloo

*Laboratoire de Chimie Inorganique, CNRS URA 420, Université Paris-Sud, 91405 Orsay Cedex, France*

Received September 17, 1998. Revised Manuscript Received February 8, 1999

The synthesis, crystal structure, electronic and second-order nonlinear optical (NLO) properties of a new bis(salicylaldiminato)nickel(II) Schiff-base complex are reported. The compound crystallizes in the space group *P1*. The NLO properties are investigated by electric field induced second harmonic (EFISH) and by INDO/SCI-SOS calculation. This compound obtained by condensation of 4-(diethylamino)salicylaldehyde and 1,2-diamino-4,5-dinitrobenzene in the presence of nickel(II) chloride exhibits the largest second-order NLO response reported for this family of bis(salicylaldiminato)nickel(II) metal complexes, with a  $\beta \times \mu$  value of  $1530 \times 10^{-48} \text{ cm}^5 \text{ esu}^{-1}$ . In addition, a thermal stability up to 300 °C, indicates potential uses of metal–salen derivatives in poled polymers matrix with high  $T_g$ .

## Introduction

Molecular-based second-order nonlinear optical (NLO) chromophores have recently attracted much interest because of their potential applications in emerging optoelectronic technologies.<sup>1–3</sup> These last 2 decades, intense activity in the field of synthetic chemistry has come from implementing molecular engineering guidelines established in the late 1970s. These efforts first focused on relatively simple “push–pull” organic chromophores with particular emphasis on the paranitroaniline family.<sup>1b,4</sup> More recently, organometallic molecules also have been investigated,<sup>5–11</sup> but very few studies have been devoted to inorganic complexes.<sup>12–18</sup> Compared to the more common organic molecules, these

complexes offer a large variety of novel structures, the possibility of enhanced thermal stability, and a diversity of tunable electronic behaviors by virtue of the coordinated metal center which might bring about NLO

(1) (a) *Molecular Nonlinear Optics*; Zyss, J., Ed.; Academic Press: New York, NY, 1994. (b) *Nonlinear Optical Properties of Organic Molecules and Crystals*; Chema, D. S., Zyss, J., Eds.; Academic Press: New York, 1987; Vols 1 and 2. (c) Prasad, N. P.; Williams, D. J. *Introduction to Nonlinear Optical Effects in Molecules and Polymers*; Wiley: New York, 1991.

(2) *Nonlinear Optical Properties of Organic Materials*; Proceedings of SPIE 1988–1994, Vols. 971, 1147, 1337, 1560, 1775, 2025, 2285.

(3) for recent reviews, see: (a) Dalton, L. R.; Harper, A. W.; Ghosh, R.; Steier, W. H.; Ziari, M.; Fetterman, H.; Shi, Y.; Mustacich, R. V.; Jen, A. K. Y.; Shea, K. J. *Chem. Mater.* **1995**, *7*, 1060. (b) Benning, R. G. *J. Mater. Chem.* **1995**, *5*, 365. (c) Special issue: Optical Nonlinearities in Chemistry. *Chem. Rev.* **1994**, *94* (1). (d) Marder, S. R.; Beratan, D. N.; Cheng, L. T. *Science* **1991**, *252*, 103. (e) Verbiest, T.; Houbrechts, S.; Kauranen, M.; Clays, K.; Persoons, A. *J. Mater. Chem.* **1997**, *7*, 2175.

(4) Williams, D. J. *Ang. Chem., Int. Ed. Engl.* **1984**, *23*, 690.

(5) For a recent reviews on NLO organometallics, see: (a) Long, N. J. *Angew. Chem., Int. Ed. Engl.* **1995**, *34*, 21. (b) Marder, S. R. In *Inorganic Materials*; Bruce, D. W., O'Hare, D., Eds.; John Wiley & Sons: New York, 1992; p 115.

(6) (a) Whittall, I. R.; Humphrey, M. G.; Persoons, A.; Houbrechts, S. *Organometallics* **1996**, *15*, 1935. (b) Whittall, I. R.; Humphrey, M. G.; Houbrechts, S.; Persoons, A.; Hockless, D. C. R. *Organometallics* **1996**, *15*, 5738. (c) Whittall, I. R.; Humphrey, M. G.; Hockless, D. C. R.; Skelton, B. W.; White, A. H. *Organometallics* **1995**, *14*, 3970.

(7) (a) Kanis, D. R.; Lacroix, P. G.; Ratner, M. A.; Marks, T. J. *J. Am. Chem. Soc.* **1994**, *116*, 10089. (b) Kanis, D. R.; Ratner, M. A.; Marks, T. J. *J. Am. Chem. Soc.* **1992**, *114*, 10338.

(8) (a) Coe, B. J.; Hamor, T. A.; Jones, C. J.; McCleverty, J. A.; Bloor, D.; Cross, G. H.; Axon, T. L. *J. Chem. Soc., Dalton Trans.* **1995**, 673. (b) Coe, B. J.; Foulon, J. D.; Hamor, T. A.; Jones, C. J.; McCleverty, J. A.; Bloor, D.; Cross, G. H.; Axon, T. L. *J. Chem. Soc., Dalton Trans.* **1994**, 3427. (c) Houlton, A.; Jasim, N.; Roberts, R. M. G.; Silver, J.; Cunningham, D.; Mcardle, P.; Higgins, T. *J. Chem. Soc., Dalton Trans.* **1992**, 2235.

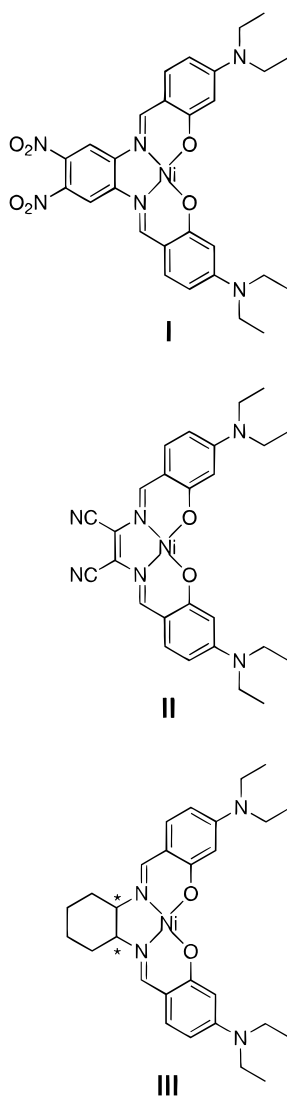
(9) (a) Loucif-Saïbi, R.; Delaire, J. A.; Bonazzola, L.; Doisneau, G.; Balavoine, G.; Fillebeen-Khan, T.; Ledoux, I.; Pucetti, G. *Chem. Phys.* **1992**, *167*, 369. (b) Balavoine, G. G. A.; Daran, J.-C.; Iftime, G.; Lacroix, P. G.; Manoury, E.; Maltey-Fanton, I.; Nakatani, K.; Delaire, J. A.; Di Bella, S. *J. Am. Chem. Soc.* Submitted.

(10) (a) Wright, M. E.; Toplikar, E. G.; Lackritz, H. S.; Kerney, J. T. *Macromolecules* **1994**, *27*, 3016. (b) Wright, M. E.; Sigman, M. S. *Macromolecules* **1992**, *25*, 6055. (c) Wright, M. E.; Toplikar, E. G. *Macromolecules* **1992**, *25*, 6050.

(11) Cheng, L. T.; Tam, W.; Meredith, G. R.; Marder, S. R. *Mol. Cryst. Liq. Cryst.* **1990**, *189*, 137.

(12) Bougault, M.; Mountassir, C.; Le Bozec, H.; Ledoux, I.; Pucetti, G.; Zyss, J. *J. Chem. Soc., Chem. Commun.* **1993**, 1623.

Scheme 1



materials with unique characteristics such as magnetic and electrochemical properties.<sup>19,20</sup>

The present paper reports on a new thermally stable donor–acceptor bis(salicylaldiminato)nickel(II) complex (Scheme 1, complex I), exhibiting a large quadratic hyperpolarizability. This molecule belongs to a class of Schiff-base complexes which have recently appeared to

be a promising family of thermally stable coordination complexes,<sup>16,17</sup> even if, to date, their NLO response was usually modest, compared to organic chromophores. The present study focuses on the synthesis, crystal structure, and second-order NLO properties of I, investigated by the electric field induced second-harmonic (EFISH) technique,<sup>21</sup> in combination with a quantum analysis within the proven INDO/SOS (ZINDO) formalism,<sup>16,17,22</sup> to describe the electronic structure and NLO property relationships of the molecule. The NLO response of I is compared to those of related II and III complexes (Scheme 1) previously reported.<sup>17</sup> Owing to the high thermal stability of metal–salen complexes, an attempt to incorporate I into poled polymer matrix is also reported.

## Experimental Section

**Materials and Equipment.** 4-(Diethylamino)salicylaldehyde was purchased from Aldrich and was used without further purification. 1,2-diamino-4,5-dinitrobenzene was synthesized according to the reported procedure.<sup>23</sup> Polyhydroxystyrene was obtained from acetoxystyrene as previously described.<sup>24</sup> II<sup>17a</sup> and III<sup>17b</sup> were prepared according to the procedure previously described. <sup>1</sup>H NMR spectra were recorded on a Bruker AM 250 spectrometer and the UV–visible spectra on a Hewlett-Packard 8452 A Spectrophotometer. Solvents (SDS or Carlo Erba) for the solvatochromism measurements were the highest purity grade and were used as supplied. 1,4-Dioxane (HPLC grade) for EFISH studies was purchased from Aldrich. The elemental analysis was performed by the Service de Microanalyses du C.N.R.S., Laboratoire de Chimie de Coordination, Toulouse, France. Thermal measurements were performed by TG/DTA analysis on a Setaram-TGDTA92 thermoanalyzer. The experiments were conducted under nitrogen on 5 mg of sample (rate of heating 10 °C/min). The decomposition temperature ( $T_d$ ) was assigned as the intercept of the leading edge of the decomposition endotherm with the baseline of the DTA scan.<sup>25</sup>

**Synthesis and Characterization of Compound I.** To a solution of 48 mg ( $2 \times 10^{-4}$  mol) of  $\text{NiCl}_2 \cdot 6 \text{H}_2\text{O}$  in absolute ethanol were successively added 40 mg ( $2 \times 10^{-4}$  mol) of 1,2-diamino-4,5-dinitrobenzene and 77 mg ( $4 \times 10^{-4}$  mol) of 4-(diethylamino)salicylaldehyde. The resulting solution was heated under reflux for 2 h, which afford I as a black precipitate. The powder was filtered off, washed with ethanol, and dried under vacuum (yield 70–75%). Anal. Calcd for  $\text{C}_{28}\text{H}_{30}\text{N}_6\text{NiO}_6 \cdot \text{H}_2\text{O}$ : C, 53.96; H, 5.17; N, 13.48. Found: C, 54.17; H, 5.52; N, 13.25. <sup>1</sup>H NMR spectrum (in DMSO- $d_6$ ): 1.262 (t,  $J = 6.9$  Hz, 12H), 3.505 (q,  $J = 7.1$  Hz, 8H), 6.059 (d,  $J = 1.8$  Hz, 2H), 6.520 (dd,  $J = 9.2, 1.8$  Hz, 2H), 7.441 (d,  $J = 9.3, 2$  Hz), 8.580 (s, 2H), 8.778 (s, 2H). Some amount of water is evidenced from IR and NMR spectra. TG analysis indicates a weight loss of 2.5% upon heating to 150 °C, which corresponds to a theoretical loss of 0.9  $\text{H}_2\text{O}$  molecules per complex. The decomposition temperature was found to be equal to 300 °C, which is consistent with the good thermal stability reported for other donor–acceptor bis(salicylaldiminato)nickel(II) complexes previously reported.<sup>16c</sup> Single crystals of I were grown by slow evaporation in 1,4-dioxane.

**X-ray Data Collection and Structure Determination.** The data were collected at 180 K on a Stoe imaging plate

(13) Zyss, J.; Dhénaut, C.; Chauvan, T.; Ledoux, I. *Chem. Phys. Lett.* **1993**, *206*, 409.

(14) Thami, T.; Bassoul, P.; Petit, M. A.; Simon, J.; Fort, A.; Barzoukas, M.; Villaeys, A. *J. Am. Chem. Soc.* **1992**, *114*, 915.

(15) Cummings, S. D.; Cheng, L. T.; Eisenberg, R. *Chem. Mater.* **1997**, *9*, 440.

(16) (a) Di Bella, S.; Fragalà, I.; Ledoux, I.; Marks, T. J. *J. Am. Chem. Soc.* **1995**, *117*, 9481. (b) Di Bella, S.; Fragalà, I.; Ledoux, I.; Diaz-Garcia, M. A.; Lacroix, P. G.; Marks, T. J. *Chem. Mater.* **1994**, *6*, 881. (c) Di Bella, S.; Fragalà, I.; Ledoux, I.; Diaz-Garcia, M. A.; Marks, T. J. *J. Am. Chem. Soc.* **1997**, *119*, 9550.

(17) (a) Lacroix, P. G.; Di Bella, S.; Ledoux, I. *Chem. Mater.* **1996**, *8*, 541. (b) Lenoble, G.; Lacroix, P. G.; Daran, J. C.; Di Bella, S.; Nakatani, K. *Inorg. Chem.* **1998**, *37*, 2158.

(18) (a) Lecours, S. M.; Guan, H.-W.; Dimagno, S. G.; Wang, C. H.; Therien, M. J. *J. Am. Chem. Soc.* **1996**, *118*, 1497. (b) Priyadarshy, S.; Therien, M. J.; Beratan, D. N. *J. Am. Chem. Soc.* **1996**, *118*, 1504.

(19) (a) Geoffroy, G. L.; Wrighton, M. S. *Organometallic Photochemistry*; Academic Press: New York, 1979. (b) Collman, J. P.; Hegedus, L. S. *Principles and Applications of Organotransition Metal Chemistry*; University Science Books: Mill Valley, CA, 1987.

(20) Kahn, O. *Molecular Magnetism*; VCH Publishers: New York, 1993.

(21) For a general discussion of EFISH technique, see: (a) Levine, B. F.; Bethea, C. G. *J. Chem. Phys.* **1976**, *65*, 2429. (b) Singer, K. D.; Garito, A. F. *J. Chem. Phys.* **1981**, *75*, 3572.

(22) Kanis, D. R.; Ratner, M. A.; Marks, T. J. *Chem. Rev.* **1994**, *94*, 195.

(23) Cheeseman, G. W. H. *J. Chem. Soc.* **1962**, 1170.

(24) (a) Arshady, R.; Kenner, G. W.; Ledwith, A. *J. Polym. Science: Polym. Chem. Ed.* **1974**, *12*, 2017. (b) Lacroix, P. G.; Lin, W.; Wong, G. W. *Chem. Mater.* **1995**, *7*, 1293.

(25) See for example: (a) Moylan, C. R.; Twieg, R. J.; Lee, V. Y.; Swanson, S. A.; Betterton, K. M.; Miller, R. D. *J. Am. Chem. Soc.* **1993**, *115*, 12599. (b) Bosnich, B. *J. Am. Chem. Soc.* **1968**, *90*, 627.

Table 1. Crystallographic Data for I

chemical formula	C <sub>34</sub> H <sub>42</sub> N <sub>6</sub> Ni <sub>1</sub> O <sub>9</sub>
formula weight	737.45
crystal system	triclinic
space group	$P\bar{1}$
crystal color	red
<i>a</i> (Å)	8.611(1)
<i>b</i> (Å)	14.154(2)
<i>c</i> (Å)	15.812(2)
$\alpha$ (deg)	113.83(2)
$\beta$ (deg)	98.50(2)
$\gamma$ (deg)	100.27(2)
<i>V</i> (Å <sup>3</sup> )	1682.1
<i>Z</i>	2
$\rho$ calcd (g cm <sup>-3</sup> )	1.46
<i>T</i> (K)	180
no. of independent reflcns ( <i>R</i> <sub>m</sub> )	5077 (0.09)
no of observed reflcns	3015
criterion for observed reflcns	<i>I</i> > 1.5 $\sigma$ ( <i>I</i> )
no. of parameters used	470
( $\Delta/\sigma$ ) <sub>max</sub>	0.02
$\Delta\rho_{\text{max}}$ (e Å <sup>-3</sup> )	0.76
$\Delta\rho_{\text{min}}$ (e Å <sup>-3</sup> )	-0.46
<i>R</i> <sup>2</sup>	0.0559
<i>R</i> <sub>w</sub> <sup>b</sup>	0.0547
GOF	1.14

$$^a R = \sum(|F_o| - |F_c|)/\sum(|F_o|). \quad ^b R_w = \sum w(|F_o| - |F_c|)^2/\sum w(F_o)^2)^{1/2}.$$

diffraction system (IPDS) equipped with an Oxford Cryosystems cooler device, with a tube power of 2 kW (50 kV, 40 mA). The crystal-to-detector distance was 80 mm. A total of 125 exposures (15 min per exposure) were obtained with  $0 < \varphi < 250^\circ$  and with the crystals rotated through  $2^\circ$  in  $\varphi$ . Owing to the rather low  $\mu x$  value (6.39 cm<sup>-1</sup>), no absorption correction was considered.

The structure was solved by direct methods (Shelxs-86)<sup>26</sup> and refined by least-squares procedures on *F*<sub>obs</sub>. Hydrogen atoms were introduced in the calculation in idealized positions (*d*(CH) = 0.99 Å) and their atomic coordinates were recalculated after each cycle. They were given isotropic thermal parameters 20% higher than those of the carbon to which they are attached. Least-squares refinements were carried out by minimizing the function  $\sum w(|F_o| - |F_c|)^2$ , where *F*<sub>o</sub> and *F*<sub>c</sub> are the observed and calculated structure factors. The weighting scheme used in the last refinement cycles was  $w = w'[1 - (\Delta F/6\sigma(F_o)^2)]^2$ , where  $w' = 1/\sum_i^4 A_i T_i(x)$  with four coefficients (*A*<sub>1</sub> = 1.19, -1.93, 0.75, -0.91) for the Chebyshev polynomial *A*<sub>1</sub>*T*<sub>1</sub>(*x*), where *x* was *F*<sub>c</sub>/*F*<sub>c</sub>(max).<sup>27</sup> Models reached convergence with  $R = \sum(|F_o| - |F_c|)/\sum(|F_o|)$  and  $R_w = \sum w(|F_o| - |F_c|)^2/\sum w(F_o)^2)^{1/2}$ , having values listed in Table 1. Criteria for a satisfactory complete analysis were the ratios of the root mean squared (rms) shift to standard deviation being less than 0.1 and no significant features in final difference maps. Details of data collection and refinement are given in Table 1.

The calculations were carried out with the CRYSTALS package programs<sup>28</sup> running on a personal computer. The drawing of the molecule was realized with the help of CAMERON.<sup>29</sup> Full interatomic distances and bond angles, fractional atomic coordinates, and the equivalent thermal parameters for all atoms and anisotropic thermal parameters for non-hydrogen atoms have been deposited at the Cambridge Crystallographic Data Center.

**NLO Measurements.** Second-order NLO measurements were carried out to reach both molecular and material properties. Molecular properties were measured by the EFISH

technique.<sup>21</sup> The light source was a nanosecond (10 ns) Nd:YAG pulsed (10 Hz) laser (B. M. Industries) operating at  $\lambda = 1.064 \mu\text{m}$ . The outgoing Stokes-shifted radiation at  $1.907 \mu\text{m}$  generated by Raman effect in a hydrogen cell (1 m long, 50 bar) was used as the fundamental beam for second harmonic generation (SHG). Further details of the experimental methodology and data analysis are reported elsewhere.<sup>30</sup> It is important to note that the calibration of our EFISH experiment necessarily implies the use of 1,4-dioxane as a solvent. In our particular case, several solutions of **I** in 1,4-dioxane with concentrations ranging from 0.5 to 2% w/w were prepared, and their SHG response was compared with that of solutions of 2-methyl-4-nitroaniline (MNA) as well as the pure solvent. For compound **II**, the solubility in dioxane being very low, the use of a mixed dioxane–chloroform (2/1) solvent was required for the detection of the SHG signal.

SHG-active polyhydroxystyrene thin films doped with **I** were prepared according to the following procedure: a few drops of a solution made from 2 mL of 1,4-dioxane, 200 mg of polyhydroxystyrene, and 10 mg of **I** were cast onto an indium tin oxide (ITO) coated glass slide. A transparent film (thickness 0.5–1  $\mu\text{m}$ ) was obtained by spin coating, and the samples were dried under vacuum for 1 day at room temperature and then for an additional day at 100 °C. The film thickness was measured with a Tencore Alpha-Step 200 surface profiler. The chromophores were poled by the following procedure: In the presence of a +600 V potential applied on a stainless grid 2 mm above the film surface and a +6 kV potential on a stainless needle approximately 1 cm above the grid, the polymer samples were heated to 160 °C for 1 h and then allowed to cool slowly to room temperature. Then, the electric potential was removed. Bulk susceptibility and its decay were measured over a period of 1 week on the same laser equipment as EFISH. A Y-cut quartz crystal (3 mm thick, *d*<sub>11</sub> = 0.5 pm/V) served as reference.<sup>31</sup>

**Calculation of NLO Response.** The all-valence INDO/S (intermediate neglect of differential overlap) method<sup>32</sup> in connection with the sum-over-state (SOS) formalism<sup>33</sup> was employed. Details on the computationally efficient INDO/SOS-based method for describing second-order molecular optical nonlinearities have been reported elsewhere.<sup>22</sup> The calculation of electronic transitions and molecular hyperpolarizabilities was performed using the commercially available MSI software package INSIGHT II (4.0.0). In the present approach, the closed-shell restricted Hartree–Fock (RHF) formalism was employed. The monoexcited configuration interaction (MECI) approximation was employed to describe the excited states. The 100 energy transitions between the 10 highest occupied molecular orbitals and the 10 lowest unoccupied ones were chosen to undergo CI mixing. Metrical parameters used for the calculations were taken from the present crystal structure of **I**.

## Results and Discussion

**Synthesis of I.** Before discussing the properties of the metal complex (NiL) **I**, it could be interesting to study the related ligand (H<sub>2</sub>L), which would provide an example of  $\Lambda$ -shaped chromophore. Such structures made of two “push–pull” subunits have been reported to exhibit enhanced hyperpolarizabilities, by the sole virtue of their two charge-transfer axis and hence large additional  $\beta$  tensor components.<sup>30,34</sup> Moreover, the in-

(26) Sheldrick, G. M. *SHELXS86, Program for Crystal Structure Solution*; University of Göttingen: Göttingen, Germany, 1986.

(27) Prince, E. *Mathematical Techniques in Crystallography*; Springer-Verlag: Berlin, 1982.

(28) Watkin, D. J.; Prout, C. K.; Carruthers, J. R.; Betteridge, P. W. *CRYSTALS Issue 10*; Chemical Crystallography Laboratory, University of Oxford, Oxford, 1996.

(29) Watkin, D. J.; Prout, C. K.; Pearce, L. J. *CAMERON*; Chemical Crystallography Laboratory, University of Oxford, Oxford, 1996.

(30) Maltey, I.; Delaire, J. A.; Nakatani, K.; Wang, P.; Shi, X.; Wu, S. *Adv. Mater. Opt. Electronics* **1996**, *6*, 233.

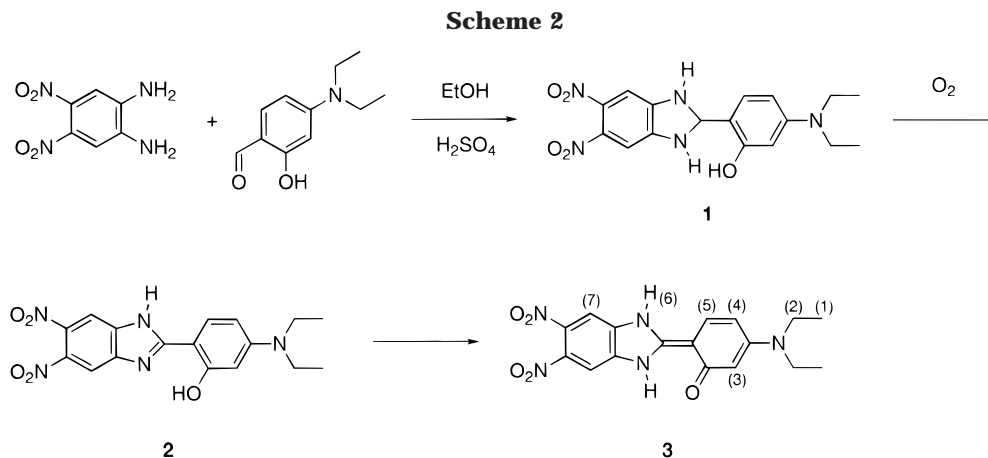
(31) Nicoud, J. F.; Twieg, R. J. In ref 1(b), Vol. 2, p 251.

(32) (a) Zerner, M.; Loew, G.; Kirchner, R.; Mueller-Westerhoff, U. *J. Am. Chem. Soc.* **1980**, *102*, 589. (b) Anderson, W. P.; Edwards, D.; Zerner, M. C. *Inorg. Chem.* **1986**, *25*, 2728.

(33) Ward, J. F. *Rev. Mod. Phys.* **1965**, *37*, 1.

(34) (a) Singh Nalwa, H.; Watanabe, T.; Miyata, S. *Adv. Mater.* **1995**, *7*, 754. (b) (a) Singh Nalwa, H.; Nakajima, K.; Watanabe, T.; Nakamura, K.; Yamada, A.; Miyata, S. *J. Appl. Phys.* **1991**, *30*, 983.





investigation of the role devoted to the metal center in **I** may benefit from the comparison between the metal complex (NiL) and the ligand (H<sub>2</sub>L), especially at the theoretical levels. Attempts to prepare the Schiff-base ligand were made by reacting 4-(diethylamino)salicylaldehyde and 1,2-diamino-4,5-dinitrobenzene, with a catalytic amount of H<sub>2</sub>SO<sub>4</sub>. This method is usually convenient, when weakly reacting amines are involved in the Schiff-base synthesis.<sup>17a,35</sup> The only result obtained along this strategy is shown in Scheme 2: a condensation takes place affording the aminor intermediate **1**, followed by an oxidation into **2**, which reorganizes in the more stable **3**. This byproduct was identified by mass spectrum and <sup>1</sup>H NMR.<sup>36</sup> Contrary to the situation observed for the H<sub>2</sub>L ligand, the NiL complex **I** was easily obtained by mixing stoichiometric amounts of the appropriate amine, aldehyde, and nickel salt. This result shows that difficulties encountered in molecular engineering of new NLO chromophores (e.g. Λ-shaped H<sub>2</sub>L) can be overcome by using a metal center, evidencing an additional role for coordination chemistry in the design of new NLO structures. No other investigations were performed in order to obtain the free H<sub>2</sub>L, for instance by removing the nickel after metal template synthesis.

**Structural Studies.** The molecular structure of **I** and atom labeling scheme are shown in Figure 1. Selected bond lengths and angles are given in Table 2. The crystal cell contains two molecules related by an inversion center, therefore canceling the second-order nonlinearity as anticipated for centrosymmetric space group *P* $\bar{1}$ . Three molecules of dioxane are present in the cell. The molecular structure reveals the same general trends observed for related Ni(II) salen derivatives, with an average metal–ligand bond lengths of 1.838(4) Å [versus 1.850(2) Å for Ni(salen)<sup>37</sup> and 1.845(4) for **III**<sup>17b</sup>] and an angle N(1)–Ni–N(2) of 86.3° (versus 86.3° and 86.5° for Ni(salen) and **III**, respectively). The nickel atom lies in a nearly perfect square-planar coordination environment with a deviation from the basal planes of

**Table 2. Bond Lengths (Å) and Angles (deg) for the Coordination Sphere of the Nickel Atom in I**

Ni(1)–Ni(1)	3.294(1)
Ni(1)–N(1)	1.842(4)
Ni(1)–N(2)	1.849(4)
Ni(1)–O(1)	1.834(3)
Ni(1)–O(2)	1.829(3)
N(1)–Ni(1)–N(2)	86.3(2)
N(1)–Ni(1)–O(1)	178.1(2)
N(2)–Ni(1)–O(1)	95.0(2)
N(1)–Ni(1)–O(2)	95.0(1)
N(2)–Ni(1)–O(2)	178.3(2)
O(1)–Ni(1)–O(2)	83.8(1)

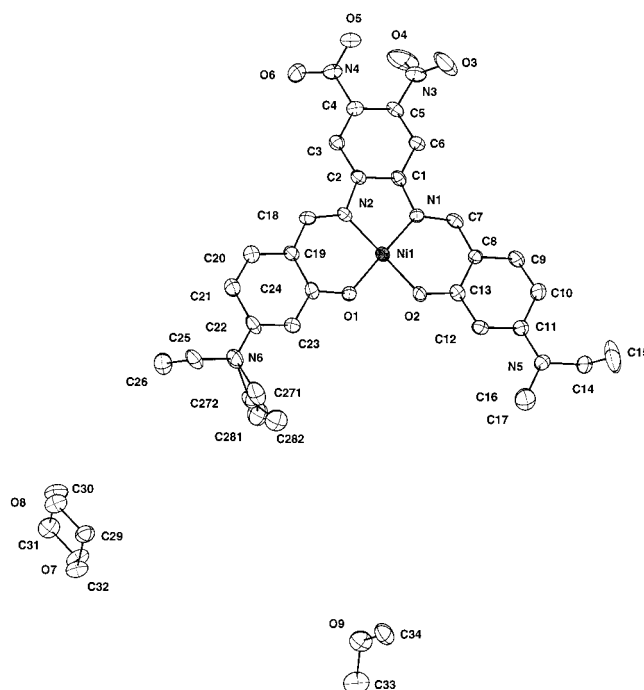


**Figure 1.** CAMERON view and atom labeling of **I**.

0.002 Å. Disorder has been treated on one terminal ethyl group (C(271), C(272), C(281), and C(282)) with restraints.

**Optical Spectroscopy and Solvatochromism.** The optical absorption spectrum of **I**, recorded in dioxane, is shown in Figure 2. The spectrum exhibits two intense bands at 536 nm ( $\epsilon_{\text{max}} = 37\,000 \text{ mol}^{-1} \text{ cm}^{-1}$ ) and 456 nm ( $\epsilon_{\text{max}} = 46\,000 \text{ mol}^{-1} \text{ cm}^{-1}$ ). Additional, less intense bands are observed at higher energy. The absorption maxima recorded in solvent of different polarities are gathered in Table 3. It can be observed that both bands

(35) Wöhrle, D.; Buttner, P. *Polym. Bull. (Berlin)* **1985**, *13*, 57.

(36) Mass Spectrum (DCI/NH<sub>3</sub>) *m/z* (% relative intensity): 372 (MH<sup>+</sup>, 100), 373 (25), 374 (6). <sup>1</sup>H NMR spectrum (in DMSO-*d*<sub>6</sub>): 1.257 (t, *J* = 6.9 Hz, 6H<sub>(1)</sub>), 3.533 (q, *J* = 6.9 Hz, 4H<sub>(2)</sub>), 3.7–4.7 (m, 2H<sub>(6)</sub>), 6.388 (d, *J* = 1.9 Hz, 1H<sub>(3)</sub>), 6.586 (dd, *J* = 9.1, 1.9 Hz, 1H<sub>(4)</sub>), 8.043 (d, *J* = 9.1 Hz, 1H<sub>(5)</sub>), 8.427 (s, 2H<sub>(7)</sub>). Hydrogen are labeled according to Scheme 2.

(37) Manfredotti, A. G.; Guastini, C. *Acta Crystallogr.* **1983**, *C39*, 863.

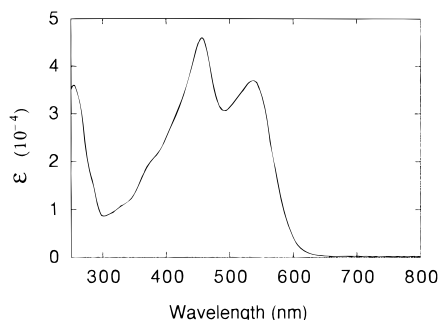


Figure 2. Optical spectrum of I, recorded in dioxane.

Table 3. Absorption Maxima ( $\lambda_{\max}$  in Nanometers) of the Two Low-Energy Optical Transitions for I, II, and III in Solvents of Different Polarities ( $E_T^N$  Reichardt Parameters)

	I		II	III	$E_T^N$
	1 → 2	1 → 3			
methanol	520	453	574	358	0.765
acetonitrile	532	456	574	358	0.472
acetone	534	456	573	360	0.355
ethyl acetate	536	456	570	361	0.577
dioxane	536	456	569	364	0.164
tetrahydrofuran	538	458	576	362	0.207
CCl <sub>4</sub>	542	462	571	370	0.090
DMSO	542	462	583	361	0.441
toluene	546	462	574	366	0.096
chloroform	548	467	582	366	0.259

exhibit a negative solvatochromism (blue shift in solvents of higher polarity). However, as observed from Table 3, this behavior seems to be a trend observed in donor–acceptor salen complexes.<sup>16,17</sup> Moreover, it must be emphasized that solvatochromism is usually associated with changes in dipole moments between the ground and the excited states upon excitation ( $\Delta\mu < 0$  in the case of negative solvatochromism). Therefore, large dipole moment changes are strongly indicative of large quadratic hyperpolarizabilities ( $\beta$ ) (vide infra). On the basis of such observations, solvatochromism has been suggested as a possible route for estimating molecular hyperpolarizabilities.<sup>38</sup> Therefore, it is interesting to compare the extent of solvatochromic shifts for complexes I, II, and III. A large number of scales have been established to quantify the influence of the solvent based on some physicochemical properties.<sup>39</sup> The Reichardt parameter ( $E_T^N$ ),<sup>40</sup> which is based on the absorption spectroscopy of a “push–pull” conjugated molecule, seems to be a suitable solvent polarity parameter, if NLO responses have to be considered. The energies of the absorption maxima are drawn in Figure 3 versus ( $E_T^N$ ). The slopes of the curves in Figure 3, which are equal to 1738, 627, and 741  $\text{cm}^{-1}$  for I, II, and III, respectively, suggest that I exhibits the largest hyperpolarizability of the series. These observations can be compared to the ZINDO-derived spectroscopic properties gathered in Table 4. Though there is a significant difference in  $\lambda_{\max}$  between calculation and experiment, the red shift while passing from III to I and II is observed at both levels.

(38) Paley, M. S.; Harris, J. M.; Looser, H.; Baumert, J. C.; Bjorklund, G. C.; Jundt, D.; Twieg, R. J. *J. Org. Chem.* **1989**, *54*, 3774.  
 (39) for a review of the solvent polarity scales, see: Buncl, E.; Rajagopal, S. *Acc. Chem. Res.* **1990**, *23*, 226.

(40) Reichardt, C.; Harbusch-Görnet, E. *Liebigs Ann. Chem.* **1983**, *5*, 721.

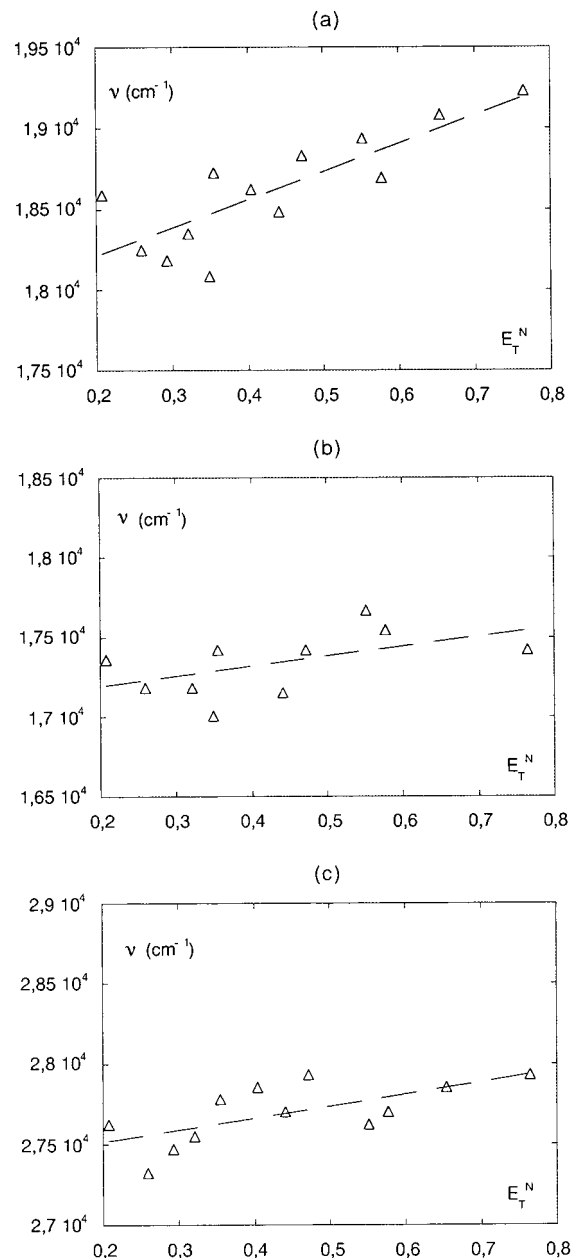


Figure 3. Solvatochromism ( $\nu$  in  $\text{cm}^{-1}$ ) for various metal–salen chromophores plotted versus the Reichardt empirical solvent parameter ( $E_T^N$ ): (a) I, (b) II, (c) III.

While the magnitude of the changes in dipole moments is consistent with the enlarged solvatochromism observed for I, the sign of the dipole moment change between ground and excited states appears to be an important issue in these systems. As already mentioned, all metal–salen-based NLO chromophores exhibit experimental negative solvatochromism, which corresponds to negative dipolar changes ( $\Delta\mu < 0$ ). Up to now, 20 metal–salen-based NLO chromophores have been reported.<sup>16,17</sup> In most cases (e.g., compound III) the ZINDO calculation confirms the negative sign. By contrast,  $\Delta\mu$  is positive for compounds I and II. This indicates that ZINDO has changed the direction of the dipole moments in the case of the diamine moieties with substituents having large withdrawing effects (this was checked for I and III, the crystal structures of which being known). Therefore, one might wonder whether in

Table 4. Experimental and ZINDO-Computed Spectroscopic and NLO Properties for I

	$\lambda_{\max}$ in nm		$\Delta\mu$ in D: calc	$\beta$ ( $\beta_{2\text{level}}$ ) at various wavelengths <sup>a</sup>							
	calc (f)	exptl ( $\epsilon \times 10^{-5}$ )		calc			exptl				
				$\beta$		$\beta_0^b$	$\mu$	$\beta_0 \times \mu$	$\beta \times \mu$		
			1.34 $\mu\text{m}$	1.907 $\mu\text{m}$							1.34 $\mu\text{m}$
<b>I</b>	436 (0.78)	536 (0.37)	6.7	107(123)	82(96)	67(79)	11.3	757		1530	968
	380 (0.69)	456 (0.46)	8.5								
	378 (0.51)		10.7								
<b>II</b>	447 (0.89)	584 (0.70)	4.3	76		41	2.9	119	1457 <sup>d</sup>	~800 <sup>e</sup>	283
<b>III</b>	328 (0.55)	358 (0.83)	-5.9								

<sup>a</sup>  $\beta$  ( $\beta_{2\text{level}}$ ) in  $10^{-30}$  cm<sup>5</sup> esu<sup>-1</sup>;  $\mu$  in D;  $\beta \times \mu$  in  $10^{-48}$  esu. <sup>b</sup> Static hyperpolarizability (zero frequency). <sup>c</sup>  $\beta_0 \times \mu$  is extracted from the experimental data assuming a two-level description (eq 1). <sup>d</sup> Data from ref 17a. <sup>e</sup> Limited accuracy ( $\pm 150$ ) due to solubility problems (see Experimental Section)

such strong acceptor containing metal–salen derivatives the ZINDO method remains fully reliable.<sup>17a</sup>

**Molecular Hyperpolarizability.** The molecular hyperpolarizability of **I** has been measured by the EFISH technique. This technique, in which the chromophores are aligned by an electric field, does not allow the determination of  $\beta$  but the projection of  $\beta$  along the dipole moment ( $\beta_{\text{vec}}$ ). However, ZINDO calculations indicate that the angle between  $\beta$  and the dipole moment ( $\mu$ ) is equal to  $3.6^\circ$  for **I**. Therefore,  $\beta$  and  $\beta_{\text{vec}}$  may be assumed to be nearly identical. The experimental  $\beta \times \mu$  value obtained for **I** is  $1530 \times 10^{-48}$  cm<sup>5</sup> esu<sup>-1</sup> (measured at 1.907  $\mu\text{m}$ ; Table 4), i.e., the largest value obtained in this class of Schiff-base compounds, although it is somewhat similar to the  $1457 \times 10^{-48}$  cm<sup>5</sup> esu<sup>-1</sup> value obtained for the previously reported **II**, using a 1.34  $\mu\text{m}$  laser radiation.<sup>17a</sup> However, it is well-known that  $\beta$ , and hence  $\beta \times \mu$ , strongly depend on the laser frequency. For instance, the two-level contribution of a  $g \rightarrow e$  charge-transfer transition depends on the laser frequency according to eq 1:

$$\beta_{g \rightarrow e} = \frac{3e^2 \hbar f \Delta \mu}{2mE^3} \frac{E^4}{(E^2 - (2\hbar\omega)^2)(E^2 - (\hbar\omega)^2)} \quad (1)$$

In this equation,  $E = \hbar\omega_{\text{eg}}$  is the energy of the charge-transfer transition,  $\omega$  is the fundamental frequency of the laser beam, and  $\beta_{g \rightarrow e}$  is the principal tensor component along the dipolar axis.<sup>41</sup> Equation 1 indicates that when  $2\omega$  is close to the absorption maxima, the dispersion factor  $E^4 / [(E^2 - (2\hbar\omega)^2)(E^2 - (\hbar\omega)^2)]$  becomes important. Consequently, the hyperpolarizability is strongly enhanced by resonance. This effect is not important for **I**, with an experimental  $\lambda_{\max}$  (536 nm) far from the 954 nm second harmonic wavelength. In the case of **II**, the experimental  $\lambda_{\max}$  (584 nm) is close to the 670 nm second harmonic wavelength, and the dispersion factor becomes important. This effect gives rise to a very large SHG response, however, artificially enhanced by resonance.<sup>17a</sup> Although this model is not the most suitable for this type of compounds (vide infra), it indicates that it is much more relevant to compare the  $3e^2 \hbar f \Delta \mu / 2mE^3$  factor in eq 1, which is the static hyperpolarizability ( $\beta_0$ ) and is independent of the laser beam frequency. The data shown in Tables 3 (solvatochromism) and 4 ( $\beta_0 \times \mu$  product) indicate that **I** exhibits a larger NLO response than that of any other metal–salen chromophore previously reported.<sup>16,17</sup> However, it

has to be noticed that the larger change in  $\beta \times \mu$  between **I** and **II** actually occurs through a dipole moment enhancement rather than a change in the hyperpolarizability. An additional experiment conducted at 1.907  $\mu\text{m}$  on compound **II** affords a  $\beta \times \mu$  value of  $800(\pm 150) \times 10^{-48}$  cm<sup>5</sup> esu<sup>-1</sup>. Although the accuracy is limited by a poor solubility and the use of a mixed dioxane–chloroform solvent, for which our EFISH equipment is not well-parametrized, this measurement confirms that the  $1457 \times 10^{-48}$  cm<sup>5</sup> esu<sup>-1</sup> value previously reported at 1.34  $\mu\text{m}$  is strongly enhanced by resonance.

These last 2 decades, a large number of organic NLO chromophores have been investigated both theoretically<sup>22,42,43</sup> and experimentally.<sup>44</sup> The principal aim of those works was first to demonstrate the adequacy of earlier models such as the two-level quantum description of charge-transfer molecules (eq 1).<sup>41</sup> In this model, the hyperpolarizability ( $\beta$ ) can be described in term of a ground and first excited-state having a charge-transfer character and is related to the energy of the optical transition ( $E$ ), its oscillator strength ( $f$ ), and the difference between ground- and excited-state dipole moment ( $\Delta\mu$ ) through the simplified relation (2)

$$\beta \propto f \Delta \mu / E^3 \quad (2)$$

However, the development of organometallic and inorganic NLO materials has been hampered by the fact that the strictly HOMO  $\rightarrow$  LUMO based two-level model frequently failed in predicting the NLO properties. This was already observed for metal–salen derivatives, where several optical transitions can be involved in the NLO response.<sup>17a</sup> Therefore, a careful examination of the  $\beta$  calculation must be conducted to fully understand the nature of the molecular orbitals involved in the nonlinearity of these materials. Details of the  $\beta$  calculation are provided in Table 4. In particular, the trend for  $\beta$  enhancement at higher frequencies can be verified, in agreement with eq 1. Within the framework of the SOS perturbation theory, the molecular hyperpolarizability can be related to all excited states of the molecule and can be partitioned into two contributions, so-called

(42) S. R. Marder, D. N. Beratan and L. T. Cheng, *Science* **1991**, *252*, 103.

(43) D. R. Kanis, Marks, T. J.; Ratner, M. A. *Int. J. Quantum Chem.* **1992**, *43*, 61.

(44) (a) Cheng, L. T.; Tam, W.; Stevenson, S. H.; Meredith, G. R.; Rikken, G.; Marder, S. R. *J. Phys. Chem.* **1991**, *95*, 10631. (b) Cheng, L. T.; Tam, W.; Marder, S. R.; Stiegman, A. E.; Rikken, G.; Spangler, C. W. *J. Phys. Chem.* **1991**, *95*, 10643.

(41) Oudar, J. L. *J. Chem. Phys.* **1977**, *67*, 446.

**Table 5. Energies ( $\lambda_{\max}$  in nm), Oscillator Strengths ( $f$ ), Dipole Moment Changes between Ground and Excited State ( $\Delta\mu$  in D), Contribution in the  $\beta_{2\text{level}}$ , and Composition of the First Excited States of **I****

transtn	$\lambda_{\max}$	$f$	$\Delta\mu$	state (%) <sup>a</sup>	composition <sup>b</sup> of CI expansion
1 → 2	436	0.78	6.7	32.7	$-0.711\chi_{109-110} + 0.394\chi_{109-112}$
1 → 3	380	0.69	8.5	24.3	$-0.381\chi_{105-118} - 0.396\chi_{109-110} + 0.431\chi_{109-111}$
1 → 4	378	0.51	10.7	22.6	$-0.667\chi_{108-110} + 0.386\chi_{108-112}$

<sup>a</sup> Contribution of the  $i$ th transition to the  $\beta_{2\text{level}}$  (state % =  $\beta_{g-e(i)}/\sum_i \beta_{g-e(i)}$ ). <sup>b</sup> Orbital 109 is the HOMO, and orbital 110 the LUMO for **I**.

two-level and three-level terms.<sup>22</sup> Analysis of term contributions to the molecular hyperpolarizability of **I** indicates that the two-level terms ( $\beta_{2\text{level}}$ ) dominate the nonlinearity (Table 4). It can mainly be related to the 1 → 2, 1 → 3, and 1 → 4 electronic transitions (Table 5). The 1 → 2 transition contributes 32.7% to the nonlinearity and essentially involves the HOMO → LUMO transition. However, additional transitions contribute significantly, which definitely indicates the inadequacy of the two-level description for these materials.

The differences in electronic population in the main three transitions involved in the NLO response of **I** are shown in Figure 4. Both diethylamino groups and nickel atoms act as electron donors upon electronic excitation, in agreement with the previous observations for **II** and **III**. However, the contribution of the diethylamino groups is modest versus that of the whole salicylaldiminato fragments. In great contrast, versus the situation encountered for **II** and **III**, the imine groups are not involved in the acceptor counterpart of the molecules, this role being mainly devoted to the two nitro substituents. Intriguingly, it can be noticed that the nitro groups are not equivalent in the charge transfer process, this difference being especially large in the 1 → 2 and 1 → 4 electronic transitions. The crystal structure can readily account for this difference. A projection of **I** along the mean plane of the molecule is shown in Figure 5. It clearly indicates that one of the nitro substituents lies out of plane. The O(4)–O(5) bond length is equal to 2.752(6) Å, which is somewhat close to the sum of the van der Waals radii (2.8 Å)<sup>45</sup> and strongly suggests that steric hindrance is responsible for this structural feature. Consequently, the contribution of this nitro substituent to the withdrawing effect is significantly reduced.

**SHG Efficiency of **I** in Poled Polyhydroxystyrene.** It is well-known that second-order NLO chromophores have to be embodied into a noncentrosymmetric environment if the molecular hyperpolarizability ( $\beta$ ) has to give rise to an observable bulk susceptibility ( $\chi^{(2)}$ ).<sup>4</sup> This can be achieved in different ways, but the most widely reported is probably the incorporation of the chromophores into polymers.<sup>46</sup> It is now generally believed that molecular second-order NLO materials will enter the marketplace, depending on the ability of the chromophores to be poled in polymers with very high glass transition temperature ( $T_g > 200$  °C).<sup>47</sup> The

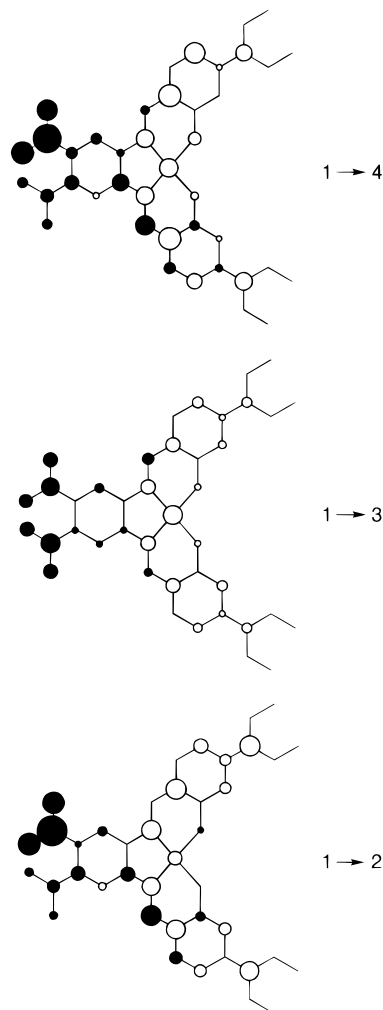


**Figure 4.** Difference in electronic populations between the ground state and the excited state for the main three transitions involved in the NLO response of **I**. The white (black) contribution is indicative of a decrease (increase) of electron density in the charge-transfer process.

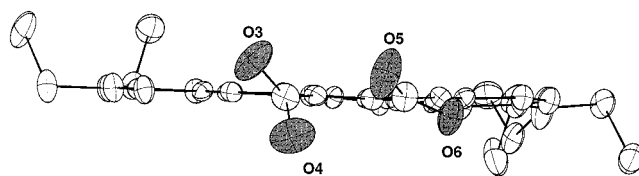


**Figure 5.** CAMERON view of **I** showing the out of plane displacement of the nitro groups.

rationale is that if  $T_g$  is around 150 °C above the device's operating temperature, the alignment will not decay significantly over the lifetime of the device. Therefore, the molecular hyperpolarizability ( $\beta$ ) will lead to an observable bulk susceptibility ( $\chi^{(2)}$ ) through relation 3

$$\chi^{(2)} = N\beta f(\omega)f(\omega)f(2\omega)O(\theta) \quad (3)$$

where  $N$  is the concentration of chromophores,  $f(\omega)$  and  $f(2\omega)$  are local field factors at  $\omega$  and  $2\omega$  frequencies, and  $O(\theta)$  is an orientation factor taking into account the position of the chromophores.<sup>48</sup> In poled polymers,<sup>49–51</sup> most of the  $\chi^{(2)}$  components vanish, and SHG measurements are usually expressed by the second harmonic

(45) *Handbook of Chemistry and Physics*, 63rd ed.; CRC Press: Boca Raton, FL, 1982; D195.

(46) *Nonlinear Optics of Organic Molecules and Polymers*, Nalwa, H. S., Miyata, S., Eds.; CRC Press: New York, 1997; 89.

(47) Dagani, R. *C&EN* **1996**, March 4, 22.

(48) Oudar, J. L.; Zyss, J. *Phys. Rev.* **1982**, A26, 2016.



coefficient  $d_{33}$  ( $=\chi^{(2)}/2$ ) through

$$d_{33} = \frac{1}{2}(N\beta F\langle \cos^3 \theta \rangle) \quad (4)$$

in which  $N$  is the concentration of the chromophores,  $F$  is the product of all local field factors, and  $\langle \cos^3 \theta \rangle = \mu E/5kT$ . It has to be emphasized that although  $\beta$  is the origin of the NLO effect, it is not the only parameter to take into account in the poled polymer response, which is proportionnal to the  $N \times \beta \times \mu$  factor. Therefore,  $\beta \times \mu$  is the molecular figure of merit for poled polymer films. Consequently, the prerequisites for achieving large and time stable efficiencies after poling are that chromophores must have large  $\beta \times \mu$  values and a very good thermal stability to endure the poling process into high  $T_g$  polymer lattices. With a  $\beta \times \mu$  value of  $1530 \times 10^{-48}$  esu (at 1.907  $\mu\text{m}$ ) and a temperature stability up to 300 °C, **I** can be compared to the best organic candidates.<sup>52</sup> With such characteristics, metal–salens such as **I** have the potential to become interesting candidates for chromophore incorporation into high  $T_g$  polymer. The  $d_{33}$  value of polyhydroxystyrene containing 5% w/w chromophore reaches 0.65 pm/V (at 1.907  $\mu\text{m}$ ), which is a sizable response for a guest–host system.<sup>53</sup> The sample retains 85% of its NLO response after 1 week, a time stability which has to be related to a glass transition temperature of 155 °C.<sup>54</sup> It is clear that larger  $d_{33}$  values ( $\approx 10$  pm/V) and a better signal stability (several months) are required if practical uses are aimed. Owing to the present experimental data, a  $d_{33}$  value of 10 pm/V would require a polymer containing  $\approx 75\%$  w/w chromophore, assuming that such a material could be poled as efficiently as a lightly doped polymer, a situation that is probably too optimistic. This high range of concentration necessarily implies the design of functionalized polymers with chromophores covalently bonded to the polymer, an approach that has also been known for providing additional time stability.<sup>46</sup> This strategy should be promising, as several metal–salen-based polymers have already been reported.<sup>35,55</sup>

(49) (a) Meredith, G. R.; Van Dusen, J. G.; Williams, D. J. *Macromolecules* **1982**, *15*, 1385. (b) Meredith, G. R.; Van Dusen, J. G.; Williams, D. J. In *Nonlinear Optical Properties of Organic and Polymeric Materials*; Williams, D. J., Ed.; ACS Symposium Series 233; American Chemical Society: Washington, DC, 1984; p 109.

(50) Williams, D. J. In ref 1b, Vol. 1, p 405.

(51) Singer, K. D.; Lalama, S. J.; Sohn, J. E.; Small, S. D. In ref 1b, Vol. 1, p 437.

(52) see for example: (a) Pushkana Rao, V.; Jen, A. K.-Y.; Chandrasekhar, J.; Namboothiri, I. N. N.; Rathna, A. *J. Am. Chem. Soc.* **1996**, *118*, 12443. (b) Dalton, L. R.; Harper, A. W.; Ghosn, R.; Steier, W. H.; Ziari, M.; Fetterman, H.; Shi, Y.; Mustacich, R. V.; Jen, A. K.-Y.; Shea, K. J. *Chem. Mater.* **1995**, *7*, 1060.

(53) Nalwa, H. S.; Watanabe, T.; Miyata, S. In ref 44, p 89.

(54) Park, J.; Marks, T. J.; Yang, J.; Wong, G. K. *Chem. Mater.* **1990**, *2*, 229.

(55) Vitalini, D.; Mineo, P.; Di Bella, S.; Fragala, I.; Maravigna, P.; Scamporrino, E. *Macromolecules* **1996**, *29*, 4478.

Another and important prerequisite will be the use of polymer backbones (e.g. polyimides) with  $T_g$  higher than 155 °C for the polyhydroxystyrene system reported in the present study.<sup>56</sup>

## Conclusion

Poling chromophores into high  $T_g$  polymer lattices has become the most promising approach toward molecular-based NLO devices. Large  $\mu \times \beta$  product and high thermal stability are important prerequisites for designing suitable candidates. Beside organic NLO chromophores, the development of organometallic chromophores,<sup>5</sup> which occasionally offer very large NLO responses,<sup>6a</sup> is hampered by usually modest thermal stabilities. On the other, intriguingly large hyperpolarizabilities have recently been reported in long-range-conjugated push–pull metalporphyrin complexes.<sup>18a</sup>

Clearly, the field of organometallic and inorganic chromophores is relatively young and unexplored. We have reported here on a new nickel(II) Schiff-base complex. Previous investigations have already pointed out several interesting aspects of this family of complexes, such as an enhancement of the second-order NLO responses by the coordination of the metal and the possibility to bring NLO materials with additional properties, by virtue of a paramagnetic center. The present study reveals more interesting properties. It is possible to bypass difficulties encountered in designing new chromophores (e.g. H<sub>2</sub>L) by using a metal center, according to the well-documented metal template synthesis procedure.<sup>57</sup> The nonlinearity of these new materials, which was rather modest compared to organic chromophores, is now strongly enhanced, the effect of the dipole moment being especially important. The properties of **I** (large  $\beta \times \mu$  value and high temperature stability), definitely establish that salen-based metal–organic species are interesting candidates for further studies and applications.

**Acknowledgment.** The authors thank Jean François Delouis for technical assistance.

**Supporting Information Available:** Full interatomic distances and bond angles, fractional atomic coordinates, and the equivalent thermal parameters for all atoms and anisotropic thermal parameters for non-hydrogen atoms. This material is available free of charge via the Internet at <http://pubs.acs.org>.

CM980650Q

(56) For recent reports on such high  $T_g$  polymers, see: (a) Yu, D.; Gharavi, A.; Yu, L. *Appl. Phys. Lett.* **1995**, *66*, 1050. (b) Verbiest, T.; Burland, D. M.; Jurich, M. C.; Lee, V. Y.; Miller, R. D.; Volksen, W. *Macromolecules* **1995**, *28*, 3005. (c) Jen, A. K.-Y.; Wu, X.; Ma, H. *Chem. Mater.* **1998**, *10*, 471.

(57) (a) *Comprehensive Supramolecular Chemistry*; Atwood, J. L., Lehn, J. M., Eds.; Pergamon Press: Oxford, 1996. (b) *Supramolecular Chemistry: Concepts and Perspectives*; Lehn, J. M., Ed.; VCH: Weinheim, Germany, 1995.